Die-Sinking by Electroerosion-Dissolution Machining

A. B. E. Khairy*; University of Alexandria/Egypt — Submitted by J. A. McGeough (1), Edinburgh University/U.K.
Received on December 1, 1989

The electroerosion-dissolution machining (EEDM) is a combination of pulsating electroerosion action aided by electrochemical dissolution. In the present study, the process is sustained for shaping small shallow dies. The kinematics of EEDM leading to the elevated rates of metal removal as well as satisfactory surface integrity and dimensional quality are identified. The machining parameters such as the specific metal removal rate, power utilization factor and die-shaping factor are evaluated experimentally and by empirical relation. The process characteristics are contrasted with electrochemical machining and electrodischarge machining processes.

Key words: Electrochemical machining, electrodischarge machining, electroerosion - dissolution machining, specific metal removal rate, power utilization factor, die-shaping factor, surface integrity.

Introduction

Many new methods of machining have been developed in recent years to deal mainly with the difficult-to-machine metals and alloys. Electrochemical machining (ECM) and electroerosion machining (EDM) are ranked as the most successful of these new methods. The two processes have been around long enough and used extensively for the machining of conventional and nonconventional materials [1,2], especially in internal machining operations such as hole drilling and die-sinking.

The pioneering work by Lazarenkos [1] on EDM in electrolytic aqueous solutions supported, over the past two decades, by experimental studies of Kubota [2] and greatly sophisticated by McGeough [3,4] to tackle many machining operations, have all led to the set up of a novel process. This process features a combined action of metal electrolytic dissolution and electric-discharge erosion. Many names were given to the combined process such as Electrochemical -discharge machining (ECDM), Electrochemical arc machining (ECAM) and Electrochemical and Electroerosion machining; a fair review for these combinations is available in [2,5].

The elevated rates of metal removal in the combined process are known to be only available because of the active electroerosion machining (EEM) phase which is estimated to be responsible for the removal of about 75 percent of the net machined stock [5]. Meanwhile, the intermittent electrochemical dissolution (ECD) phase aids in metal removal and helps improving the surface quality [6]. The dominant effect of erosion action in the combined EEM-ECD process suggests the process to be rather called as Electroerosion-dissolution machining (EEDM).

Like the pure ECM and EDM, EEDM can be used for turning, drilling and die-sinking operations. In nonconventional processes the die-sinking is an operation which should be distinguished from hole drilling. The former usually involves machining over a relatively large contoured area with the main interest in surface quality of bottom walls of die cavity. The machine tool used for die-sinking should be rigid enough to withstand high hydrodynamic and electromagnetic forces exerted in the machining zone, and usually equipped with high rating electrolyte pumping unit and heavy duty power generator. for hole drilling, light machines in terms of rigidity and power requirements are used since the rate of metal removal is eventually smaller than in die-sinking and surface finish of side walls is of most concern [7].

This paper is a preliminary empirical study of die-sinking by EEDM. The process kinematics leading to higher rates of metal removal are discussed briefly. Simple machining parameters are developed to reveal the trend of process with various combinations of machine variables. Typical surfaces and geometries produced by EEDM in Stainless Steel dies are presented.

Theoretical description of process kinematics

Recent theoretical and experimental investigations have dealt with the characteristics of electrical discharging in ECM electrolytes, for single pulsed and multiple pulsed power sources [8,9]. The shape of input pulsed power was also studied, especially the rectangular and sinusoidal shapes [9,10]. The discharge action in liquid electrolytes is always accompanied with electrochemical action. The two actions may occur in-phase or out-phase depending upon conditions dominating in the machining gap between tool and workpiece. The principal variables involved in hybrid EEDM process rendering the generation of electrical discharges and electrolytic dissolution are shown in Fig.1. While electrochemical dissolution is spontaneously occuring in the gap medium, erosion by electrical discharges will come about and aid metal removal.

With respect to the distribution of machining actions along the machining gap, Fig.2 shows that region A is likely to be tackled merely by ECD, region C is machined mainly by EEM and intermediate region B by a combination of ECD and EEM. This specific classification of working phases in EEDM is eventually based upon the intergap spacing between cathode and anode which controls the field concentration and current density. The die geometry along the side walls is also divided into three parts; the entrance part (I), the taper part (II) with length L, and the die-bottom part (III).

Test rig and experimental conditions

A schematic diagram is shown in Fig.3 for the test rig used in experiments. The rig is composed of five main arrangements:

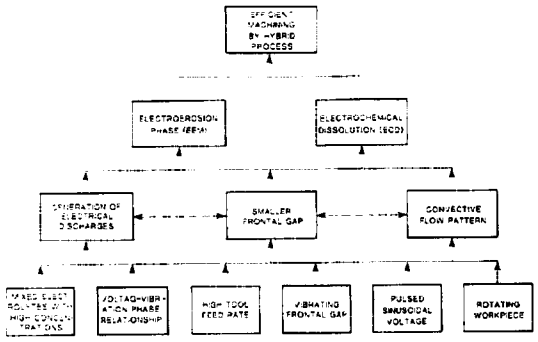

Fig.1 Principal controllable variables of EEDM.

1. An electric power supply unit which generates DC pulsed sinusoids of 10 ms periodic time. The unit was capable of supplying up to 200 A at 15 to 50 v. An over - current protection for short circuit was devised to minimize any harmful effects that may rise on tool or workpiece.
2. An electrolyte system to pump the electrolyte through a machining gap built up between cathode and anode electrodes. A flowmeter and pressure gauge were implemented to control the hydrodynamics of electrolyte flow along with a clarifier to clear off the machining debris.
3. Electrode tooling to clamp, and sometimes rotate, the cathodic tool, convey the pumped liquid through or to tool and precisely setting the workpiece.
4. A machine base and control console which combined the above mentioned items as a rigid machine tool. The control console enabled control over the machine variables which include the average open gap voltage, cathode oscillation amplitude, cathode feed rate, phase shift between pulsed input voltage and cathode oscillation waveforms.
5. A measurement rack that directly measured the following quantities, a) the weight loss from tool and workpiece, b) the amount of coulomb, c) the consumed power, and d) the actual machining time.

The feed of cathode tool through workpiece was achieved by a stepper motor triggered by a chopper drive, thereby feed rates of 0.5 mm/min to 28 mm/min were obtainable. The starting position of cathode in-feed was set by a linear rule whereas the travelling depth was measured via a dial indicator. The depth of blind sink was limited to about 30 mm which was

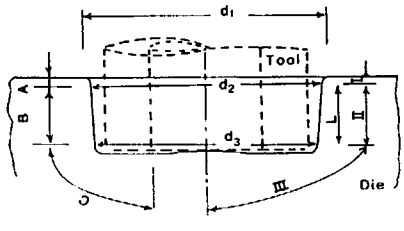

Fig.2 Die sections and machining regions.

* Present Address: Department of Mechanical Engineering, Sultan Qaboos University, P.O.Box 32483, Al-Khod, Oman.

accurately set through the die by accounting for tool wear by EEM effects.

Tools were made of commercial bronze piping of 9.4 mm and 3.7 mm diameters (The alloy specifications: 90% Cu and 10% Zn,and specific weight 8.3 gm/cm^3). The workpiece material was rolled plates 316 Stainless Steel of 40 mm thickness. Sodium Chlorate ($NaClO_3$) electrolyte of 120 g/l was used as a machining medium because it is noncorrosive and known to produce high surface finish and controlled geometrical tolerances when devoted to ECM applications [10]. The electrolyte flow rate was assumed constant at 7.2 m/s when coupled with a stationary pumping pressure of 0.8 MPa.

During machining the coulomb-meter and power-meter were set into counting their respective quantities as cumulative number of pulses. Each one of these pulses has a precalibrated value which was thereafter multiplied by the total number of pulses counted at the end of a machining run. A two channel digital oscilloscope has been connected to a current simulator box and power terminal to capture records of passing current and machining power respectively, as exhibited in Fig.3. After every run the loss in tool and workpiece weights were measured by a weigher. The diameters were measured by internal micrometer at three different levels of die circumference. The workpiece samples were then sawed into longitudinal and cross sections, ground down to plane surfaces and etched for further metallugraphic and dimensional tests.

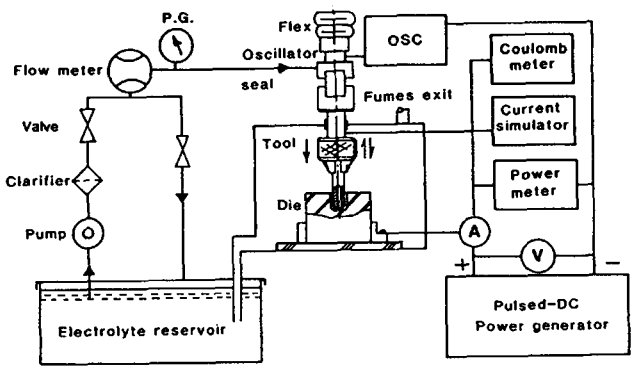

Fig.3 A shematic of EEDM die-sinking.

Machining parameters

A simplified method based on the Faraday's principle of electrolysis will be employed here to develop some important machining parameters. The validity of these parameters, however, is limited to the physical and electrochemical conditions indicated herewith for every case. First we develop the following simple parameters

- The average diameter of die (d_a). This parameter is defined by

$$d_a = [\text{Volume of metal removed/Die depth} \cdot \pi/4]^{1/2}, \text{ or}$$

$$d_a = 2\,[m/\pi\rho h]^{1/2} \qquad (1)$$

where m is the removed stock from workpiece (gm), ρ is its specific mass (gm/mm^3) and h is the die depth (mm).

- The current density (j). If the electrolysis current efficiency (η) is assumed to be constant at any reported value, then from the Faraday's law of electrolysis

$$I = m/\ \eta\ t\ e_a \qquad (2)$$

where I is the electrolysis current (A), t is the machining time (s) and e_a being the electrochemical constant (g/C). The momental current density j (A/cm^2) throughout the whole surface area engaged in machining (the tremendous current density in plasma channel of discharge erosion is ignored) will be.

$$j = I/s \qquad , s = d_a.h$$

Therefore, from (1)

$$j = (1/2\ \eta\ e_a t)\,[m\ /\ \pi h]^{1/2} \qquad (3)$$

Appendix (A) shows the composition and electrochemical properties of 316 Stainless Steel. The chemical equivalent of the alloy is 26.41 g, hence, the electrochemical equivalent is 27 x 10^{-5} g/C. It is assumed that the valency of alloy is fixed and will not be changed during machining, especially in transition between polarization states (If it is assumed that the only expected EC reaction at the work surface will be metal dissolution, the current efficiency (η) may reasonably be assumed to be 100%).

On substitution in (3) by these values, and with h= 30 mm,hence

$$j = 1740\ m/\eta t \qquad (4)$$

The current density at any moment of machining time can be found by considering the partial derivatives of both variables in eq.(4).

Now, the following three machining variables will be developed.

1. The specific metal removal rate (smrr). This is directly assessed from the ratio between removed volume of workpiece metal and amount of Coulomb registered by the Coulomb-meter during machining, that is for the given data,

$$smrr = 23.55.\ d_a^2/c \qquad (5)$$

where smrr (mm^3/KC) and c is the total amount of Coulomb on meter (C).

2. The power utilization factor (puf). This variable is designed to rate the volume of metal removed from the die-cavity (mm^3) to the total amount of power (q) counted up by power meter (Kj), i.e.,

$$puf = 23.55\ .\ d_a^2/q \qquad (6)$$

This value of puf can implicitly be estimated for any machining setting by assessing smrr in (5) and from the meter readings of c and q, thus

$$puf = smrr.\ c/q \qquad (7)$$

3. The die-shaping factor (dsf). The die-shaping factor is a measure of conicity in die cylindrical shape, and estimated by

$$dsf = (d_2 - d_3)/L \qquad (8)$$

The diameters d_2 and d_3 are measured at two sections shown as levels I and II in Fig.2 and L is the vertical height between these two sections. The dsf parameter can be used to compare the geometry of die shapes produced by EEDT and its candidates: the pure ECM and EDM. The average die diameter d_a can also be a useful shape comparative parameter since machining by ECM is usually accompanied with a certain taper in die sides; EDM has similar but smaller effect and EEDM is expected to produce dies of intermediate characters between the two processes.

Experimental results and power equation

The whole trend of relationship between the governing variables and machining parameters in EEDM can be represented by power equations. Only two governing variables were studied, namely the tool feed rate and the average applied voltage across machining gap; the machining parameters included smrr, puf and dsf. The individual and mutual influences of the governing variables on machining parameters are tested by analysis of variance, prior to developing power equations. These were found afterwards by treating the governing variables as independent input variables with power exponents and the machining parameters as dependent output variables. The exponent constants were estimated by linearizing the equations and finding best estimates for constants by error minimization techniques [11].

The feed rate was set at five different levels 3, 6, 12, 15 and 18 mm/min and the average applied voltage at three levels 20, 25 and 30 v. Thus, a 15 full-factorial experiments were conducted while keeping all other variables fixed. Table 1 shows the various combinations of governing variables, calculated and measured parameters and machining parameters.

The following relationship is developed for smrr from experimental data

$$smrr = 0.83(\text{Feed rate})^{1.083}.(\text{Average voltage})^{0.352} \qquad (9)$$

The actual data collected from experiments are given in column 8 of Table 1, denoted as EXP. In column 9 the values predicted by eq. (9) are given alongside denoted as PRED. It is evident that predictions made by power equation (9) are very close to experimental data values. However, it is deducible from eq.(9) that smrr is directly proportional to both variables, the feed rate and average voltage. Moreover, the power exponent of the former indicates much powerful influence on smrr than the latter.

TABLE 1 EXPERIMENTAL CONDITIONS AND DATA FOR EEDM-DIE SINKING

No	Ave. Voltage (v)	Feed rate (mm/min)	CALCULATED & MEASURED PARAMETERS d_a (mm)	j (A/Cm^2)	C (KC)	q (KJ)	Smrr (mm3/KC) EXP.*	PRED**	puf (mm3/KJ)	dsf (mm/mm)
1		3	14.09	183.71	550.20	060.01	08.50	07.83	78.00	0.19
2		6	13.82	179.52	277.80	064.68	16.16	16.67	69.60	0.15
3	20	12	13.24	174.90	128.40	086.01	32.17	35.18	48.00	0.13
4		15	12.10	145.75	079.80	081.02	43.18	44.84	42.60	0.12
5		18	11.05	104.42	052.20	119.86	55.01	54.51	26.40	0.11
6		3	12.78	172.61	471.00	087.86	08.17	08.50	43.80	0.12
7		6	12.31	154.52	178.20	112.19	20.00	18.17	31.80	0.09
8	25	12	11.77	137.18	075.60	126.52	36.17	38.00	21.60	0.07
9		15	11.19	134.53	063.00	098.35	46.84	48.51	30.00	0.05
10		18	10.54	132.09	045.60	090.85	57.34	59.01	48.00	0.05
11		3	17.05	181.37	805.20	158.53	08.50	09.00	43.20	0.15
12		6	15.22	151.11	318.00	154.20	17.17	19.17	35.40	0.15
13	30	12	11.93	106.65	081.60	133.03	41.17	40.67	25.20	0.10
14		15	10.47	106.68	051.60	056.68	49.84	50.18	45.60	0.10
15		18	9.98	184.11	039.60	095.35	58.84	63.01	24.60	0.09

(OTHER CONDITIONS: CURRENT EFFICIENCY 100%, OSCILLATION AMPLITUDE 0.2 MM AND PHASE ANGLE ZERO DEGREE)

* EXP. DENOTES smrr FROM EXPERIMENTAL DATA, CALCULATED BY EQ.(5)

** PRED. DENOTES smrr PREDICTED BY POWER EQ.(9)

Like in conventional ECM and EDM, the machining components in EEDM, i.e. EEM and ECD, are intensified by higher feed rates. The frontal machining gap tends to be smaller and the flow rate of electrolyte is consequently accelerated. Likewise, the pulsed voltage will help agitating the electrolyte, gases and debris mixture which stabilizes the machining action by EEM and ECD[6,9].

Fig.4 shows the effect of feed rate on the die-average diameter, d_a, for three average voltages 20, 25 and 30 v. The decrease in d_a with increased feed rate is visible especially for the highest average voltage; a 41% decrease in d_a (This decreased from about 17 mm to 10 mm) occured when feed rate is increased six folds (from 3 mm/min to 18 mm/min). This suggests a mode of metal removal mainly by ECD component up to the maximum attainable feed rates by pure ECM, i.e. 6 mm/min, in similar machining conditions [12]. The rest of metal should have been removed by EEM component. It is also evident from Fig.4 that machining at the intermediate voltage, 25 v, has produced not only the smallest rate of variation in d_a with feed rate, but more remarkably also the smallest d_a values. The findings of this particular machining condition are

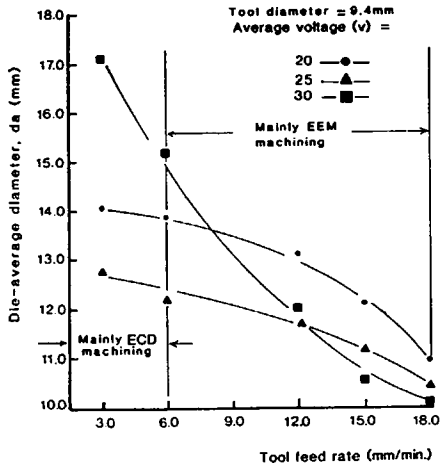

Fig.4 Variation in die-average diameter with tool feed in different voltages.

reproduced in Fig.5 with an extra coordinate, the current density j, for further explanations. The two (or double) sided overcut in die diameter is shown to diminish with higher feed rates, so does the current density. This last parameter is calculated merely from Faraday's principle of electrolysis, eq. (3), while the experimental values are for the combined ECD - EEM components. Hence, the values of current density are interpreted to account for EEM effect in current density rating higher than these commonly known for ECD in comparable conditions. The j values are shown in Fig.5 to be considerably high in lower feed rates (in the range 3 to 6 mm/min), a discrepancy which could be attributed on one side to the electrochemical reactions at higher feed rates (which is usually accompanied with smaller frontal gaps), with a possibility of changing from active to transpassive dissolution modes. On the other side, the incredibly condensed current densities in EEM plasma channels over infinitely small times can not be measured by provided provisions. Later discussions on surface integrity will explain these effects further.

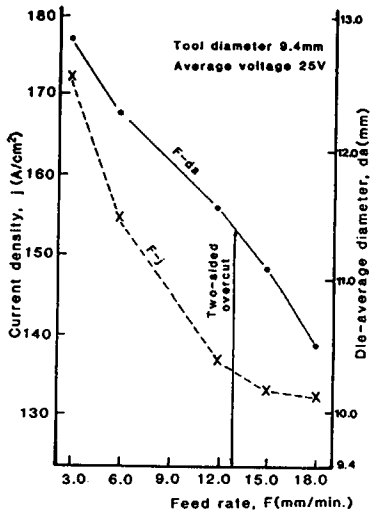

Fig.5 Effect of tool feed-rate on current density and die-average diameter with average voltage 25 v.

The promotion in smrr with elevated rates of feed rate can be seen from plots in Fig.6. Higher voltages have signified greater rates of metal removal. The high accuracy of eq. (9) in representing the experimental data can be judged from the typical example shown for machining at average voltage 20 v.

Broadly speaking, the frontal machining gap in EEDM should be much smaller than that in pure ECM, for fixed feed rates. This situation endures because of substantial pollution of machining gap by machining products [6,13], and also the application of pulsed rather than constant DC voltage [4,9]. Smaller frontal gaps always entail higher current densities for ECD. The generation of electrolytic gases in liquid and formation of oxide films on workpiece surface seem both to deviate this tendency of high current density. EEM can now be activated by electrical discharges between cathode and anode rather than between the two electrodes and gas voids [2,8]. The amount of energy absorbed by the tool and usually causes tool wear can also impair the process of metal removal from workpiece. The ratio of metal volumes removed from tool and workpiece was in the range of 1 to 27%, for the present experimental combinations, which is almost double EDM rates but with much higher feed rates.

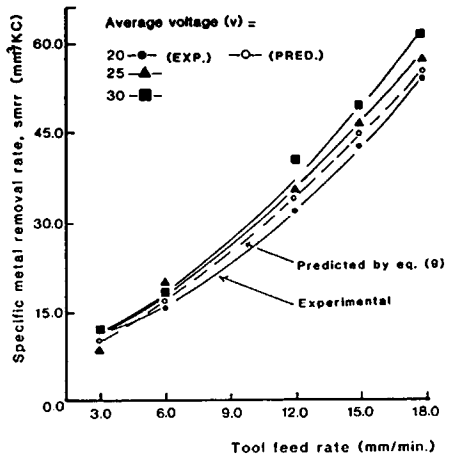

Fig.6 Variation in Smrr with tool feed-rate for three voltages.

The exponent of average voltage in eq.(9) can be seen to be less than unity which implies that at higher values of this variables the rate of rise in smrr will be smaller; Fig.7 shows a verification for this condition if comparing the ordinates S_1 and S_2. The reduced efficiency in ECD component with increased average voltage could be the reason. In this case the high levels of voltage have exerted lower current density and smaller die diameter (Table 1), with a greater contribution of EEM action. The 3-D representation in Fig.7 shows assessment for variation in power utilization factor (puf) when machining at the minimum and maximum feed rates 3 and 18 mm/min. The smaller feed rate has shown a significant drop in puf with increased voltage, almost one-half of its original high value. This behavior is attributed, as pointed out before, to electrolytic reactions likely to occur with higher voltages which favour EEM at the expense of ECD. The plot for higher feed rate, 18 mm/min, supports this claim since it showed little variation in puf due to prevailing EEM action.

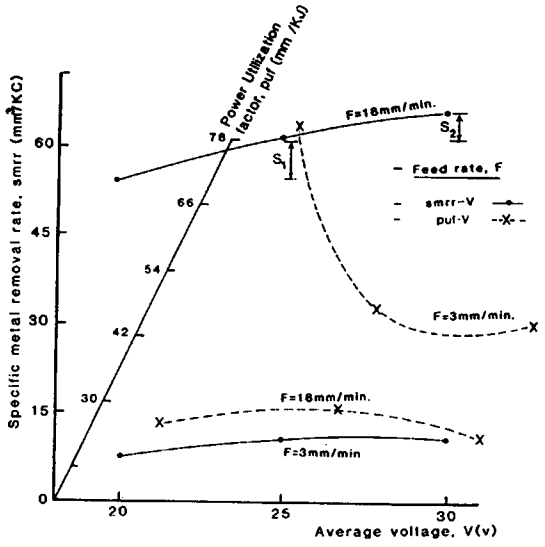

Fig.7 3-D representation of relationship of Smrr, puf and average voltage at lowest and highest feed-rates.

The variant behavior of smrr and puf parameters can be justified by the difficulties arising in understanding the way by which machining power is consumed in high rates of electrolysis and erosion machining [12,13]. This phenomenon is particularly pronounced in situations whereby the effects arising from several gap variables may act adversely, as is the case for EEDM components.

The last column in Table 1 lists values of the die-shaping factor (dsf) as calculated by eq. (8). Apparently there is a decrease in dsf with increased feed rate, for all levels of machining voltage. As indicated before, the dsf reflects, to some extent, the degree of conicity in cylindrical shape assumed for die. Such a cylindrical shape is subjected to a widening effect by stray ECD of the highly pumped electrolyte at exit end (top side) of the die. Concurrently the EEM action continues working mainly at the frontal machining zone that always corresponds to die bottom; Fig.2. The machining at intermediate average voltage, 25 v, seems to have been optimum with all combinations of feed rate of since it yielded the smallest dsf value. Fig.8 demonstrates this criterion for a typical feed rate 12 mm/min. The other feed rates have shown a similar trend. At 25 average

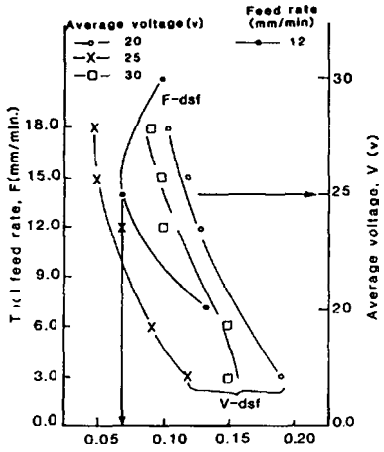

Fig.8 Variation in dsf with average voltage and optimum feed-rate of 12 mm/min.

voltage there was probably a good balance between factors leading to side machining and those working at the frontal gap. Since the former is mainly due to ECD stray machining, the passive layer covering the side walls of die tends to transform into a transpassive one in that particular high voltage. The concentration of electric fields in the frontal gap in this case will become moderate enough so that a steady course of erosion (mainly by spark pulses) is taking place locally. The study of surface integrity in next section can elucidate the surfaces conditioned by ECD and EEM actions for this particular machining condition.

It might have been realized that puf and dsf can be expressed in terms of feed rate and voltage by power relationships similar to that developed for smrr, eq.(9). Both parameters, however, have shown elegant and clear relationships with the input governing variables as discussed above.

Surface integrity for parts produced by EEDM should include a study of the metallurgical and mechanical alternations that may occur in the surface layers. The combination of ECD and EEM in EEDM produces interinsic effects on machining products, surface roughness, shape geometry and subsurface layers. The procedure used to investigate the surface integrity is similar to that used to analyse the drilling of heat-resistant alloys by ECAM process [15].

Metal hydroxide and spherical droplets of oxidised metal were found in the spent $NaC10_3$ electrolyte. These residues are respectively indicatives of ECD and EEM components. The molten craters on workpiece surface, formed by severe thermal erosion pulses, are quenched very rapidly in the surrounding cold electrolyte. The surface and subsurface layers will quickly undergo metallurgical phase transformations. Hollow metallic spheroids formed by the ejected molten metal are suspended in the liquid. The size of these spheroids was between 5 and 310 μm compared with 1-210 μm for EDM spheroids. Fiercer thermal erosion pulses in EEDM are the reason for the larger size of spheroids.

The mode of metal removal by ECD is known to be function of the kind of surface films formed at anodic surface that could be active, selective, passive or transpassive. The good dimensional control when machining in $NaC10_3$ electrolyte is due to the behaviour of surface films which could change from active to passive to transpassive modes with elevated voltage. The change from passive to transpassive mode of metal removal occurs suddenly with every small potential change on polarization curve. Thus the dimensional control by ECD phase in $NaC10_3$ electrolyte is exercised by building up of a thick passive film at areas of low potential, i.e. side walls of die, which gradually transits to a thin electronically conductive (transpassive) film at area of high potential in the frontal machining gap.

The EEM pulses act selectively too over the workpiece surface. Metal is removed from die stock by preferential erosion process which means that nearest peaks between tool and workpiece are machined first. The randomly located erosion pulses would rupture the anodic passive film if

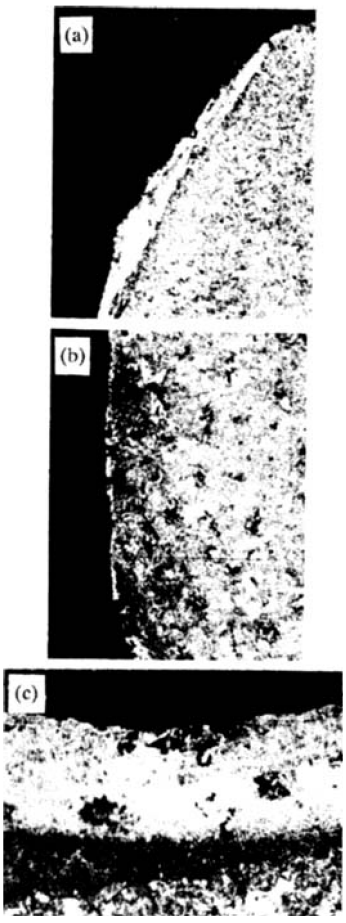

Fig.9 Optical microscopy sections at die entrance (a), midheight (b), and central bottom (c).

struck along side walls of die and produce mat-cratered surface at the frontal gap zone.

At the entry top of die between d_1 and d_2, as shown in Fig.2, a rounded filleted surface existed for all specimens with fillet radius of typically 0.7 to 1.1 mm. The early damaged surface layer by EEM when tool starts to penetrate through blank surface is gradually recessed by prolonged ECD stray action. The second section exhibited a constantly tapered shape (height d_2-d_3 or L). The value of that taper is given by dsf parameter in Table 1 and ranged between 0.05 and 0.19 mm/mm. This range of die taper by EEDM is of a value between the wider ECM range and the closer EDM range in comparable current density and power levels. By now the white damaged layer (also called the recast layer), normally caused by EEM metal melting and redepositing on the surface, would start to appear along the die sides. The thickness of that layer is consistently decreasing in the direction of electrolyte up-stream owing to the continuous attack by ECD. this last action in $NaC10_3$ has also caused high pitting to the overall die surface. The thickness of white layer ranged between 0 and 130 μm, and shown to be dependent upon the tool feed rate and to a lesser extent the applied voltage. Finally, the die bottom section had shown relatively thicker damaged layer because of concentrated EEM action in frontal gap. The layer thickness jumped to a range of 8 to 280 μm for machining respectively at average voltage 30 v-feed rate 3 mm/min as well as average voltage 20 v-feed rate 18 mm/min. The heat affected-zone thickness was shallowest (140 μm) at the former condition and deepest (288 μm) in the latter condition. Fig.9 shows an example of optical microscopy sections at entry (a), midheight (b) and central bottom (c) of die surface.

Microcracks and macrocracks were also observed in the white layer, occasionally extended to the annealed sub layer. Most of the microcracks were dissolved by ECD action and some of the macrocracks withstood dissolving especially at highest level of feed rate and applied voltage. The pitted surface of die by selective ECD action is shown in Fig.10(a) which was repeatedly observed over the surface sides. Fig.10(b) shows the white damaged layer by EED action at the die bottom section, with clear cracks of the micro and macro sizes.

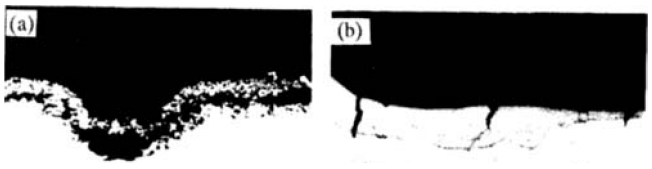

Fig.10 Pitted surface by ECD at die side walls (a) and white damaged layer with micro and macro cracks(b).

Conclusions

Die-sinking by EEDM process of 316 Stainless Steel alloy is feasible regarding metal removal rate, dimensional tolerances and surface integrity. Metal removal rate is considerably higher than pure ECM and EDM processes, dimensional tolerances are controllable than ECM and comparable with EDM, and the surface integrity reflects ECM-EDM effects. High sinking (feed) rates were obtainable in the range of 3 to 18 mm/min when machining with pulsed DC voltage of average value 20 to 30 v and in 120 g/l $NaC10_3$ electrolyte. The limits of machining parameters developed from experimental data for the given settings are: the specific metal removal rate: 8.17 - 58.84 mm^3/KC, the power utilization factor 24.60 - 78.00 mm^3/KJ, and the die-shaping factor 0.05 - 0.19 mm/mm.

The effect of increasing tool feed rate on these machining parameters was positvely proportional, except for the last parameter. Average applied voltage has shown effects inferior to feed rate but still proportional to the first two parameters and developed optimum conditions for die-shaping factor at 25 v.

A power equation was developed for relating the specific metal removal rate and machine governing variables, the feed rate and average voltage. Surface pitting by ECD action and heat-affected zone, with micro and macrocraks, by EEM action were found on surface and subsurface layers.

Acknowledgements

The experimental facilities and funds that made available by the Department of Production Engineering of Alexandria University were essential for completion of this work. Thanks are due to Professor A.E. Al-Ashram, Head of the Department. Many thanks are also due to Professor S.M. Soliman for helpful discussions and to Professor H.A. Awad for sincere guidance.

Appendix (A)

The chemical composition and electrochemical properties of 316 St/St were as follows [7].

Element	%	Atomic Weight	Assumed valency (Other valency)	Chemical Equivalent
Fe	66	55.85	2 (3)	27.93
Cr	17	51.99	3 (2,6)	17.34
Ni	12	58.71	2 (3)	29.36
Mo	03	95.94	3 (4,6)	31.98
Mn	02	54.94	2 (4,6,7)	27.47

The electrochemical equivalent of alloy is 27×10^{-5} g/C.

References

[1] Lazarenko, B. and Lazarenko, N., "Mechanism of Passage of Electric Current Through Electrolytes", Elektronnaya Obrabotle Materialov, N.1, 5-10, (1979).

[2] Kubota, M., "Metal Removal in ECDM", Proc. ISEM - 217-220, (1977).

[3] Drake, T. and McGeough, J., "Aspects of Drilling by Electrochemical Arc Machining", Proc. Machine Tool Design Conf., MacMillan Pub., 362-369, (1981).

[4] El-Hofy, H., and McGeough, J., "Evaluation of an Apparatus for Electrochemical Arc Wire - Machining"., Trans. ASME, J.of Eng. for Indust. V110, 119-123, (1988).

[5] Khairy, A., "Stochastic Analysis of Electroerosion-Dissolution Turning", Proc. of The Twentieth Annual Pittsburgh Conf. on Modelling and Simulation., V2, 268-174, (1989).

[6] McGeough, J., Khairy, A. and Munro, W., "Theoretical and Experimental Investigation of the Relative Effects of Spark Erosion and Electrochemical Dissolution in ECAM"., Annals of the CIRP V 32/1, (1983).

[7] Chryssolouris, G, and Wollowitz, M., "Electrochemical Hole Making", Annals of the CIRP, V 33/1, 99-104, (1984).

[8] Ryblko, A. and Zaydman, G., "The Energy Possibility of Pulse Electrochemical Machining of Metals", Electro. obr. Mat., 17-20, (1979).

[9] Ryblko, A., "Single-Pulse Generator for Studying ECM of Metals with Pulse Industrial Current", Electrochemistry in Industrial Processing and Biology, N.5, 79-80, (1978).

[10] Chikamori, K, Yamomoto, H. and Ito, S., "stoichmetric Investigation of Electrochemical Machining", J. of Electrochemical Society, 118, 68-72, (1980).

[11] Holman, J., "Experimental Methods for Engineers", McGraw-Hill, 4th Ed., (1987).

[12] Loutrel, S. and Cook, N., "High Rate ECM Machining"., Trans. ASME., 950, 992-996, (1973).

[13] Crichton, I. et al, "Comparative Studies of ECM, EDM & ECAM", J.of Precision Eng., U.K., V 141, 155-160, (1981).

[14] Bartel, E. and Hockenberry, T., "The Arc Phenomenon in Electrical Discharge Machining and its Effects on the Machining Process"., Conf. of Methods of Machining, Forming and Coating, IEE, 18-20 Nov., 125-131, (1975).

[15] A Private Report to the Rolls Royce Ltd, Bristol, No.MPI-85, (1981).